Journal of Organometallic Chemistry 716 (2012) 110–119

Contents lists available at SciVerse ScienceDirect

Journal of Organometallic Chemistry

journal homepage: www.elsevier.com/locate/jorganchem

Synthesis, molecular structure and electrochemistry of gold(I) complexes with 1-(diphenylphosphino)-1′-[(diphenylphosphino)methyl]ferrocene

Petr Štěpnička*, Ivana Císařová

Department of Inorganic Chemistry, Faculty of Science, Charles University in Prague, Hlavova 2030, 12840 Prague, Czech Republic

ARTICLE INFO

Article history:
Received 5 June 2012
Received in revised form
12 June 2012
Accepted 12 June 2012

Keywords:
Ferrocene ligands
Phosphines
Gold(I) complexes
Structure elucidation
Electrochemistry

ABSTRACT

Depending on the reaction stoichiometry, 1-(diphenylphosphino)-1′-[(diphenylphosphino)methyl]ferrocene (**1**) reacts with [AuCl(tht)] (tht = tetrahydrothiophene) to afford an insoluble polymer formulated as $[\mathrm{AuCl}(\mathbf{1})]_n$ (**2**) or ligand-bridged digold(I) complex, $[(\mu\text{-}\mathbf{1})(\mathrm{AuCl})_2]$ (**3**). The latter compound readily undergoes metathesis reactions with anionic reagents such as *in situ* generated acetylides, thiocyanate or *N*,*N*-diethyldithiocarbamate to give the corresponding digold(I) complexes $[(\mu\text{-}\mathbf{1})(\mathrm{AuY})_2]$, where Y is C≡CPh (**4**), C≡CFc (**5**; Fc = ferrocenyl), SCN (**6**), and $\mathrm{Et_2NCS_2}$ (**7**). Similar reaction of **3** with a dithiolate formed from propane-1,3-dithiol and sodium methoxide affords a macrocyclic bis-chelate $[(\mu\text{-}\mathbf{1})(\mathrm{AuSCH_2CH_2CH_2SAu})]$ (**8**). Compounds **2**–**8** have been characterized by spectroscopic methods (multinuclear NMR, ESI, MS, UV–vis and IR) and by elemental analysis, and the molecular structures of $\mathbf{3}\cdot\frac{1}{2}\mathrm{C_2H_4Cl_2}$, $\mathbf{4}\cdot 2\mathrm{CHCl_3}$, $\mathbf{7}\cdot 2\mathrm{CHCl_3}$, and **8** have been determined by single-crystal X-ray diffraction analysis. Cyclic voltammetric study revealed that ligand **1** undergoes a one-electron oxidation at the ferrocene unit, which is associated with some chemical complications resulting presumably from the presence of the lone electron pair at phosphorus. After coordination to Au(I)L fragments bearing simple auxiliary ligands (e.g., in **3**, **4**, and **6**), the $\mathrm{Fe^{II}/Fe^{III}}$ redox process becomes reversible and appears shifted to more positive potentials owing to an electron density transfer from the diphosphine ligand to the coordinated metal centers. For compounds **5** and **7**, this redox change is accompanied by additional waves attributable to oxidation of ferrocenyl groups in the terminal ferrocenylethynyl groups and to redox changes occurring at the Au-bound carbamate ligands, respectively.

1. Introduction

The somewhat stagnant coordination chemistry of gold(I) [1] has recently revived due to the discovery of new interesting structures, fundamentally attractive gold–gold closed-shell interactions [2] and, mainly, because of numerous applications of gold(I) complexes in materials research [3], homogeneous catalysis [4] and biomedicine [5]. As a soft metal ion forming usually stable linear coordination assemblies, gold(I) has been also utilized as a defined building block for the preparation various coordination arrays [6] via substitution and complexation reactions, being often combined with ferrocene-based metalloligands. The majority of Au(I)–Fe(II) complexes [7] has been obtained from the ubiquitous 1,1′-bis(diphenylphosphino)ferrocene (dppf) [8]. Compounds resulting from ferrocene monophosphines such as $\mathrm{FcPPh_2}$ (Fc = ferrocenyl) [9], $\mathrm{FcCH_2PPh_2}$ [10], $\mathrm{FcCH_2P(CH_2OH)_2}$ [11] and $(\mathrm{FcC{\equiv}C})_n\mathrm{PPh}_{2-n}$ ($n = 1,2$) [12] remain still less common.

In view of our previous studies aimed at understanding the coordination behavior of ferrocene-based P,N-donors possessing an inserted methylene group (A and B in Scheme 1) toward Au(I) [13], we decided to also include in testing the recently reported semi-homologous dppf congener **1** [14] (Scheme 1). This study describes the preparation of a bis(chlorogold(I)) complex from this unsymmetric diphosphine ligand and its further reactions with anionic reagents to give a series of trimetallic $\mathrm{Au_2Fe}$ complexes. Also reported are a detailed structural characterization of these newly prepared compounds by means of spectroscopic methods and single-crystal X-ray crystallography, and investigations into their electrochemical properties.

2. Results and discussion

2.1. Synthesis and spectroscopic characterization

Initial reaction tests were aimed at understanding the course of the reactions occurring in the **1**–[AuCl(tht)] system (tht = tetrahydrothiophene). To this end, appropriate amounts of

---

* Corresponding author. Fax: +420 221 951 253.
E-mail address: stepnic@natur.cuni.cz (P. Štěpnička).

0022-328X/$ – see front matter © 2012 Elsevier B.V. All rights reserved.
http://dx.doi.org/10.1016/j.jorganchem.2012.06.007

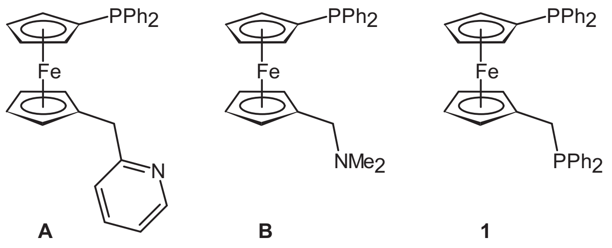

Scheme 1.

these starting materials were dissolved in $CDCl_3$ and the reaction mixtures were monitored by ^1H and $^{31}P\{^1H\}$ NMR spectroscopy. When mixed at a 1:1 M ratio, the starting materials quickly dissolved to produce a clear yellow solution, which then slowly deposited a fine yellow precipitate. NMR spectra recorded shortly after mixing revealed a single Au–Fe compound to be formed along with liberated tht (Fig. 1). The ^{31}P NMR signals of the product were markedly broadened, probably due to dynamic processes. The yellow solid product, which separated almost completely after standing at 4 °C overnight (86% isolated yield at 20 μmol scale), was isolated and analyzed as a 1:1, probably polymeric complex [AuCl(**1**)] (**2**). It should be noted that formation of an intermediate [AuCl(*PP*)] complex and its easy polymerization to give $[AuCl(PP)]_n$ was noted earlier for dppf (=*PP*) [7f,7g], and that a defined molecular [AuCl(*PP*)] "intermediate" was later isolated upon replacing dppf with its bulky permethylated analogue, $[Fe(\eta^5\text{-}C_5Me_4PPh_2)_2]$ [15].

A similar reaction of **1** with two equivalents of [AuCl(tht)] (Au:P = 1:1) afforded a clear deep yellow solution, which also contained a single product according to the NMR spectra (Fig. 1). This product was identified as the expected bis(chlorogold) complex **3** (Scheme 2).

Repeating the later reaction at a larger scale produced a good yield of the air-stable yellow complex **3**, which was used as a convenient entry to other Au(I)–Fe(II) complexes via metathesis-like reactions with various anionic reagents (Scheme 2). Thus, treatment of **3** with *in situ* formed sodium acetylides, sodium thiocyanate and sodium *N*,*N*-diethyldithiocarbamate afforded bis(η^1-alkynyl) complexes **4** and **5**, Au(I)-thiocyanate **6** and carbamate **7**, respectively. Similar reaction of **3** with propane-1,3-ditiolate gave a 13-membered trimetallamacrocycle **8**, for which a counterpart can be found in the chemistry of dppf [16].

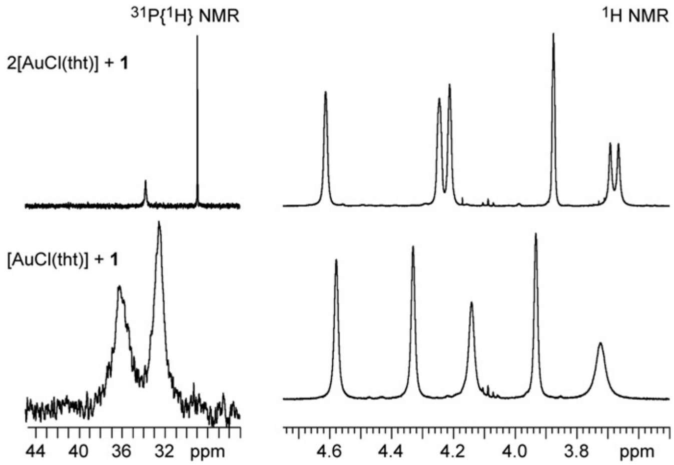

Fig. 1. $^{31}P\{^1H\}$ NMR (left) and ^1H NMR (right) spectra of reaction mixtures prepared by mixing [AuCl(tht)] with diphosphine **1** at 1:1 (bottom) and 2:1 (top) molar ratios in $CDCl_3$. For ^1H NMR spectra, only the region of ferrocene and CH_2 protons is shown for clarity. The signals in the $^{31}P\{^1H\}$ NMR spectrum of *in situ* generated **3** (shown on top) have different widths but integrate to the same intensity.

Compounds **3**–**8** were isolated as yellow, air-stable solids and were characterized by elemental analysis, ^1H and $^{31}P\{^1H\}$ NMR spectroscopy, UV–vis spectroscopy and by electrospray ionization (ESI) mass spectrometry. In addition, the crystal structures of four representatives were determined by X-ray crystallography and the whole series of Au(I) complexes except for insoluble **8** was studied by cyclic voltammetry.

In the ^1H NMR spectra, compounds **3**–**8** displayed four resonances due to the chemically non-equivalent protons at the ferrocene-1,1′-diyl unit, a multiplet of the phosphine phenyls and a characteristic doublet of the PCH_2 group ($^2J_{PH}$ = 10–11 Hz). For **3**–**7**, the methylene signal was seen in a rather narrow range δ_H 3.57–3.72, while in the case of **8**, it appeared shifted to considerably

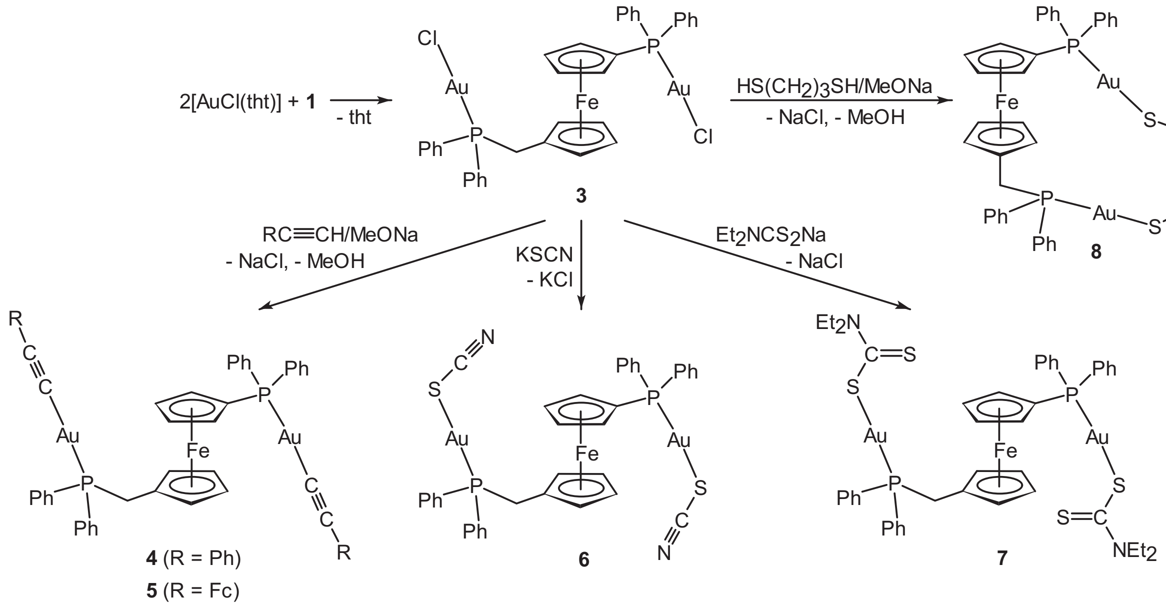

Scheme 2. Synthesis of compounds **3**–**8** (Fc = ferrocenyl).

higher fields (δ_H 2.79). The ^{1}H NMR spectra further exhibited signals due to the anionic ligands, namely characteristic multiplets of the phenyl and ferrocenyl groups for **4** and **5**, respectively, signals of to the virtually equivalent ethyl groups in **7**, and signals of the trimethylene bridge in the macrocyclic complex **8**. The ^{31}P NMR spectra of **3**–**8** showed two resonances (singlets) for the non-equivalent phosphorus atoms. The positions of these signals varied upon changing the 'terminal' donors attached to Au(I) with δ_P increasing with increasing *trans*-influence [17] of the terminal ligand (δ_P: **3** < **7** < **6** < **8** < **4** ≈ **5**). Finally, the presence of the thiocyanato ligands in **6** was clearly manifested in the IR spectrum through a pair of diagnostic bands at 2120 and 2076 cm^{-1} [18].

With the exception of compound **7**, the positive-ion ESI mass spectra of all molecular Au(I) complexes displayed intense signals at *m*/*z* 765 corresponding to [Au(**1**)]$^+$ (N.B. Only this signal was observed for compound **6** under standard conditions). In contrast, the spectrum of compound **7** showed only ions resulting via elimination of one anionic ligand (*m*/*z* 1110). In addition to the mentioned ion at *m*/*z* 765, the spectra of **3**–**5** and **8** exhibited signals attributable to the molecular and/or pseudomolecular (e.g., [M + Na]$^+$) ions and ions resulting by elimination of one terminal ligand (chloride or acetylide; not possible for **8**).

The UV–vis spectrum (Fig. 2) of complex **3** recorded in 1,2-dichloroethane consisted a composite band tailing off from the UV region. Compounds possessing terminal ligands capable of π-conjugation displayed more intense bands shifted toward lower energies. For instance, the dithiocarbamate complex **7** showed at strong band at 265 nm and a composite band extending to longer wavelengths (with a maximum at ca. 292 nm). In the case of acetylide **5**, the "main" band was shifted to 292 nm while the phenylethinyl analogue **4** showed a composite band consisting of a pair of sharp, intense bands at 270 and 284 nm, a relatively weaker band at 258 nm and a shoulder around 293 nm. Even these bands were accompanied by relatively weaker bands extending toward lower energies.

2.2. Molecular structures

The formulation of compounds **3**, **4**, **7** and **8** was unequivocally corroborated by single-crystal X-ray diffraction analysis for solvates for **3**·½$C_2H_4Cl_2$, **4**·2$CHCl_3$, **7**·2$CHCl_3$ and **8** isolated after recrystallization as specified in the Experimental section. Views of the molecular structures are presented in Figs. 3–5 and 7. Pertinent geometric data are given in Table 1.

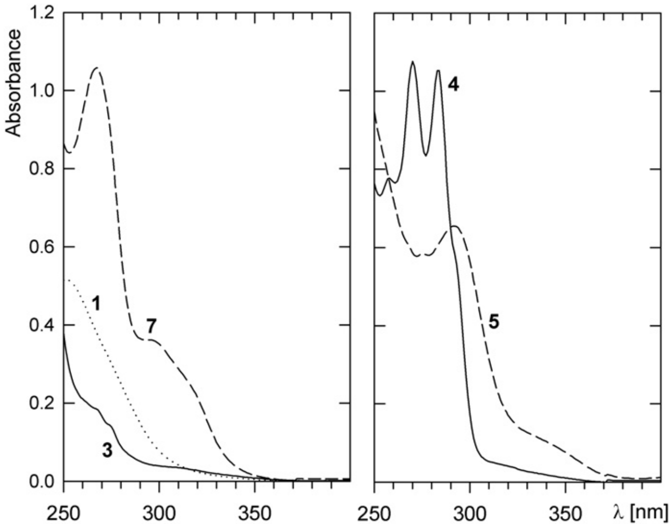

Fig. 2. UV–vis spectra of ligand **1** and complexes **3**, **4**, **5** and **7** as recorded for ca. 2 × 10^{-5} M solutions in 1,2-dichloroethane (optical path 1.0 cm).

The Au-donor bond lengths in **3** compare well with those reported earlier for [(dppf)(AuCl)$_2$] [7a,7m,19], [(FcCH$_2$PPh$_2$)AuCl] [10] and for phosphine–AuCl complexes obtained from phosphinoferrocene pyridines [13a] and phosphinoamine **B** (Scheme 1) [13b]. The two Au–P distances in **2** are practically identical. The Au–Cl bond lengths differ by only ca. 0.01 Å, the shorter Au–Cl bond and the wider P–Au–Cl angle being associated with Au2 connected to the less encumbered CH$_2$PPh$_2$ group.

The structure of **4** reveals nearly linear coordination for both Au(I) ions. The geometry of P–Au–acetylide fragments is similar to that reported for [(μ-dppf)(AuC≡CFc)$_2$] [20] and complexes of the type [(FcPPh$_2$)AuC≡CR], where R = Fc, 4-C_6H_4CN, 2,5-bis(*N*,*N*-dimethylaminomethyl)-4-iodophenyl and 2,2′-bipyridine-3-yl [9b]. Likewise, parameters describing the coordination geometry of **7** do not depart much from those reported for [(R_3P)Au(dtc)], where R = phenyl [21] and 2-tolyl [22], and for the dppe-bridged complex [(μ-dppe){Au(dtc)}$_2$] (dppe = 1,2-bis(diphenylphosphino)ethane, dtc = *N*,*N*-diethylcarbamodithioato) [23].

In **7**, the versatile dtc ligands [24] coordinate in essentially monodentate fashion. This is particularly evident in the case of Au1 showing unlike Au1–S1/2 distances (Au1–S1 2.337(1) Å, Au2–S2 3.047(1); cf. the sum of the covalent radii being 2.38 Å [25]). For Au2, this bond asymmetry is significantly lower (Au2–S3 2.3559(9) Å, Au2–S4 2.918(1) Å), which in turn corresponds with a more pronounced delocalized character of the CS_2^- moiety bonding to Au2 (cf. the difference in the C–S bond lengths being ca. 0.06 and 0.03 Å for dtc ligands attached to Au1 and Au2, respectively). The close approach of the second sulfur atom to the Au(I) centers is further reflected by a closure of the P–Au–S angles (ca. 172° for both Au1 and Au2) [26].

An inspection of the data presented in Table 1 reveals that the Au–P bond distances increase with increasing *trans*-influence [17] of the other ligand coordinated to the gold(I) center (i.e., **4** > **8** > **7** > **3**). It is also noteworthy that the molecules of **3**, **4** and **7** bearing simple terminal ligands share the overall molecular conformation (see Fig. 8 and torsion angles in Table 1 [27]). In all three cases, the PPh$_2$ group attached directly to the ferrocene unit is oriented so that the P1–Au1–donor arm points toward the ferrocene unit with Au1 located on the side accommodating the methylene spacer. The methylene group linking the second phosphinogold moiety is approximately perpendicular to the plane of its parent ring Cp2 and the P2–Au2–donor arm extends away from the ferrocene core and from Au1.

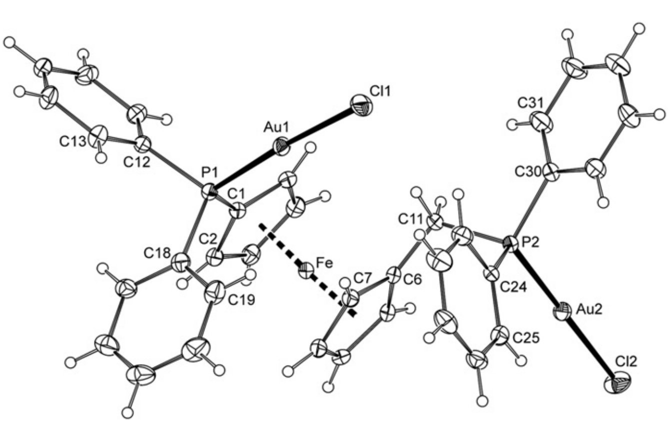

Fig. 3. View of the complex molecule in the crystal structure of **3**·½$C_2H_4Cl_2$. Displacement ellipsoids correspond to the 30% probability level.

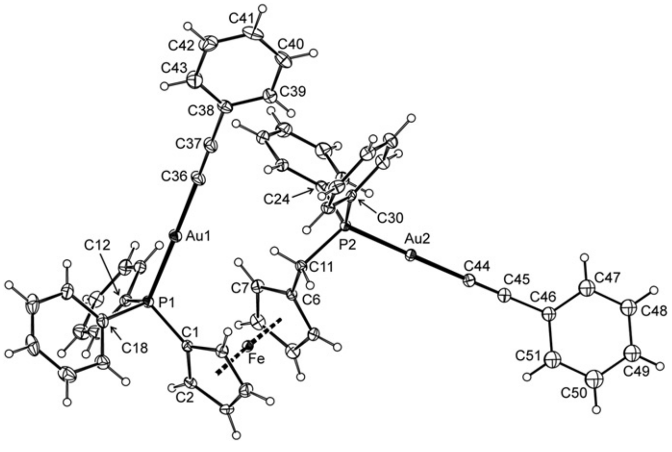

Fig. 4. View of the complex molecule in the structure of **4**·$2CHCl_3$. Displacement ellipsoids correspond to the 30% probability level. Only one position of the disordered phenyl ring C(46–51) is shown for clarity.

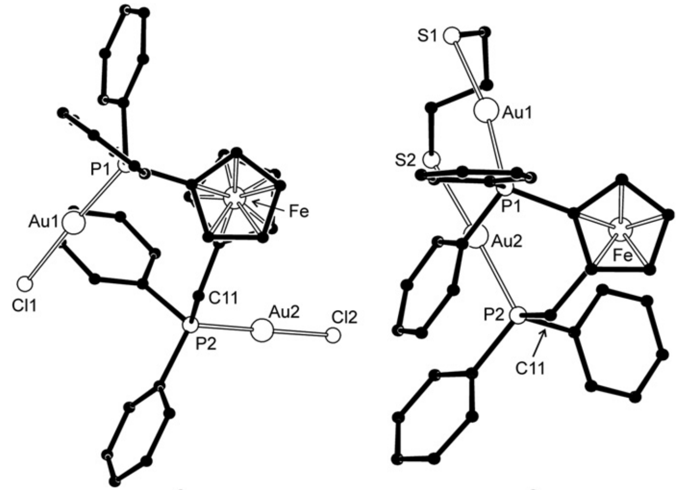

3 **8**

Fig. 6. Views of the molecules of **3** and **8** in the Cg1···Cg2 direction (i.e., along the axis of the ferrocene moiety). Hydrogen atoms are omitted for clarity.

Ferrocene units in the molecules of **3**, **4** and **7** are regular and assume conformations close to synclinal eclipsed (cf. the ideal value $\tau = 72^\circ$). Surprisingly, the most pronounced departure from the regular geometry is seen for complex **3** featuring monoatomic terminal ligands. This compound shows the largest tilt angle (ca. 4°) and its substituents are the most distant in the series due to the largest mutual rotation of the cyclopentadienyl rings.

Despite the presence of a relatively short bridge, the structure of ferrocenophane-like compound **8** (Fig. 7) remains undistorted with the interatomic distances and angles falling within the usual ranges. For instance, the individual Au–P and Au–S distances in **8** are similar to each other and compare well with the data reported for the dppf analogue $[(dppf)(AuSCH_2CH_2CH_2SAu)]$ [16,28], which can be expected to be more strained owing to an absence of the flexible methylene spacer. The P–Au–S angles in **7** depart from linearity by ca. 10° (Au1) and 6° (Au2), which is less than in the dppf analogue showing the P–Au–S angles of ca. 165°.

The overall molecular conformation of **8** differs from that found for the compounds with non-bridging terminal ligands discussed above. As shown in Fig. 6 the ferrocene cyclopentadienyls remain close to synclinal eclipsed and the CH_2PPh_2 group is oriented above the ferrocene unit. However, the C11–P2 bond is inclined toward P1 (cf. C7–C6–C11–P2 angles in Table 1) and the P2–Au2–S2 arm and one of the phenyl groups at P2 are found in mutually interchanged positions. As a result, both gold atoms are located on one side of the ferrocene unit with the vectors of the Au–P bonds being close to parallel, thus facilitating the closure of the macrocycle. Notably, the conformation of **8** differs from that observed for the dppf analogue in which the cyclopentadienyl rings adopt a synclinal eclipsed conformation while the P–Au–S arms are arranged in a staggered manner, thereby allowing for an intramolecular aurophilic contact (Au···Au ≈ 3.06 Å) [29].

It is also noteworthy that with the exception of complex **3**, the compounds studied do not form any significant intra- or intermolecular aurophilic contacts [2] in the solid state (Au···Au ≥ ca. 5 Å). In the case of complex **3** (Fig. 8), the Au1 atoms from proximal molecules related by the crystallographic two-fold axis are involved in a weak aurophilic interactions with Au1···Au1′ distance of 3.2502(2) Å, which is shorter than double the van der Waals radius (ca. 3.32 Å [25]). The torsion angles X–Au1–Au1′–X′ are 108° for both X = Cl and P. The second shortest intermolecular contact in the structure of **3** is detected between Au2 atoms in a

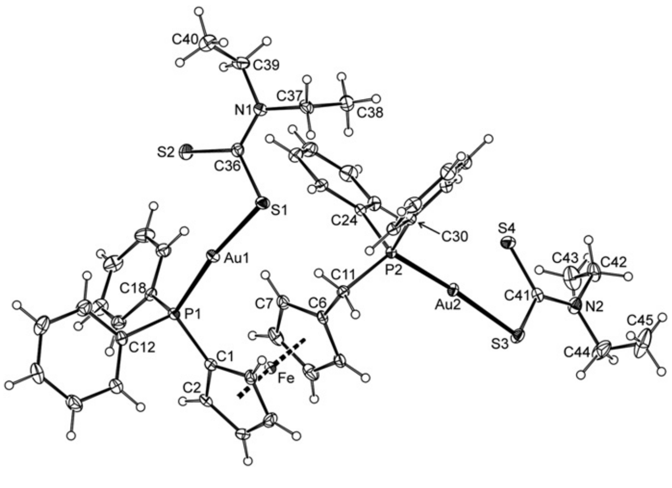

Fig. 5. View of the complex molecule in the structure of **7**·$2CHCl_3$ showing displacement ellipsoids at the 30% probability level.

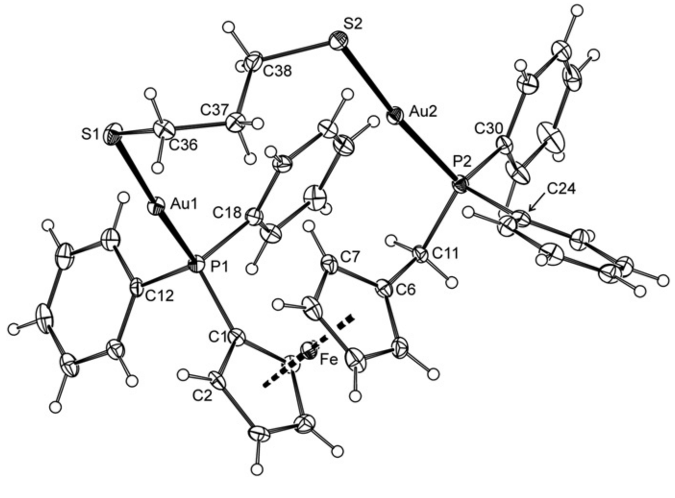

Fig. 7. View of the molecular structure of **8**. Displacement ellipsoids are scaled to 30% probability level.

Table 1
Selected distance and angles (in Å and deg) for **3**·½$C_2H_4Cl_2$, **4**·2$CHCl_3$, **7**·2$CHCl_3$, and **8**.

Parameter[a]	**3**·½$C_2H_4Cl_2$	**4**·2$CHCl_3$[e]	**7**·2$CHCl_3$[f]	**8**[g]
X/Y	Cl1/Cl2	C36/C44	S1/S3	S1/S2
Au1–P1	2.233(1)	2.272(1)	2.2495(9)	2.2612(8)
Au1–X	2.296(2)	1.999(6)	2.337(1)	2.2896(9)
P1–Au1–X	175.29(5)	177.7(2)	171.98(3)	170.24(4)
Au2–P2	2.231(1)	2.272(1)	2.2459(9)	2.2702(9)
Au2–Y	2.286(2)	2.012(4)	2.3559(9)	2.287(1)
P2–Au2–Y	177.02(5)	178.8(1)	172.12(3)	174.08(4)
Au1···Au2[b]	7.6959(3)	7.2537(2)	7.4143(2)	5.4181(2)
C7–C6–C11–P2	91.2(5)	−94.4(4)	−91.7(4)	66.4(4)
C6–C11–P2–Au2	59.4(4)	−62.4(3)	−62.4(3)	−55.1(3)
C5–C1–P1–Au1	−24.9(4)	34.2(4)	26.5(4)	−144.6(3)
P1–Au1/P2–Au2	104.51(5)	97.40(4)	99.66(4)	161.70(4)
Fe–Cg1	1.643(2)	1.650(2)	1.642(2)	1.648(2)
Fe–Cg2	1.648(2)	1.648(2)	1.648(2)	1.651(2)
tilt[c]	4.4(3)	1.7(3)	1.3(2)	0.6(2)
τ[d]	88	76	75	70

[a] Definition of the parameters: Cp1 = C(1–5), Cp2 = C(6–10). Cg1 and Cg2 are the respective ring centroids.

[b] Intramolecular distance Au1···Au2.

[c] Dihedral angle of the least-squares planes of the cyclopentadienyl rings.

[d] Torsion angle C1–Cg1–Cg2–C6.

[e] Further data: C36–C37 1.203(8), Au1–C36–C37 173.3(5), C44–C45 1.186(4), Au2–C44–C45 176.2(3).

[f] Further data: Au1–S2 3.047(1), S1–Au–S2 65.82(3), Au2–S4 2.918(1), S3–Au2–S4 67.49(3), C36–S1 1.755(4), C36–S2 1.697(4), S1–C36–S2 119.7(2), C36–N1 1.337(5), C41–S3 1.737(4), C41–S4 1.705(4), S3–C41–S4 119.0(2), C41–N2 1.328(5).

[g] Further data: S1–C36 1.822(4), C36–C37 1.519(5), C37–C38 1.506(5), S2–C38 1.836(4), Au1–S1–C36 108.7(1), S1–C36–C37 116.9(2), C36–C37–C38 113.6(3), C37–C38–S2 114.8(3), C38–S2–Au2 108.1(1).

molecule and its inversion-related image. However, the Au2···Au2′ distance of 4.2162(3) Å exceeds the sum of the van der Waals radii, which is in accordance with an unfavorable antiparallel orientation of the P–Au–Cl units resulting from the imposed symmetry.

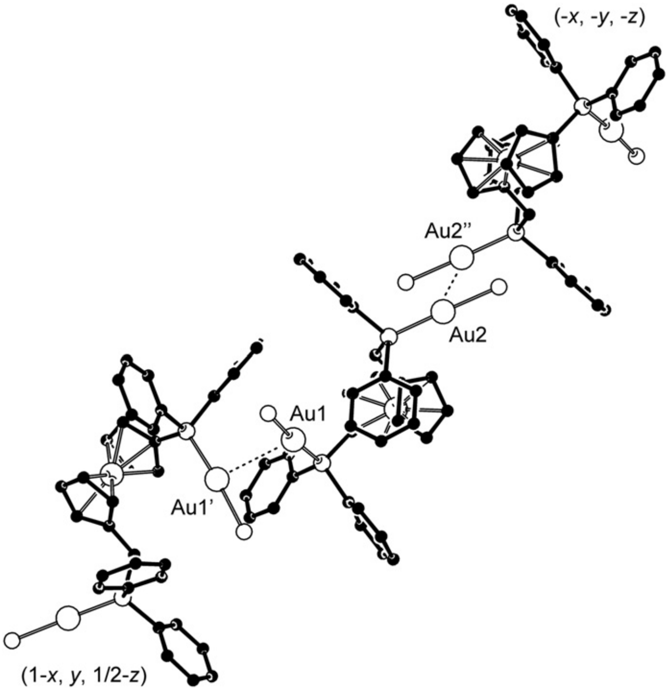

Fig. 8. Partial packing diagram for **2** showing the shortest intermolecular Au···Au contacts as red dotted lines. The hydrogen atoms were omitted for clarity. The interatomic distances are as follows: Au1···Au1′ = 3.2502(2) Å, Au2···Au2″ = 4.2162(3) Å.

Table 2
Summary of electrochemical data for **1**–**6**.[a]

Compound	$E^{0\prime}$ [V]	Compound	$E^{0\prime}$ [V]
1	0.070	**5**	−0.005,[c] 0.370
3	0.400	**6**	0.425
4	0.365[b]	**7**	ca. 0.445[d]

[a] The redox potentials were determined as an average of the anodic (E_{pa}) and cathodic (E_{pc}) peak currents in cyclic voltammograms and are given relative to ferrocene/ferrocenium. For details, see Experimental.

[b] The redox process is complicated by adsorption phenomena.

[c] Oxidation of the terminal ferrocenyl groups.

[d] The ferrocene-based oxidation is accompanied by other redox changes (see text). In addition, an irreversible reduction is observed at E_{pc} = 0.795 V.

2.3. Electrochemistry

Anodic electrochemistry of compounds **1** and **3**–**7** was studied by cyclic voltammetry at platinum disc electrode in dichloromethane solution containing 0.1 M $Bu_4N[PF_6]$ as the supporting electrolyte. Compound **8** could not be analyzed due to an insufficient solubility [30]. Pertinent data are presented in Table 2.

Free ligand **1** expectedly undergoes a single one-electron oxidation attributable to the electrochemically reversible ferrocene/ferrocenium couple (Fig. 9). However, this redox event is associated with chemical reactions, which make the overall redox response quasi-reversible and produce some electroactive products giving rise to additional waves at higher potentials. As a result, the ratio of the anodic and cathodic peak currents (i_{pa}/i_{pc}) increases with increasing scan rate (ν; Fig. 9). Otherwise, the primary redox change represents a standard diffusion-controlled process as indicated by the anodic peak current increasing with the square root of the scan rate ($i_{pa} \propto \nu^{1/2}$).

Such behavior is not unprecedented among ferrocene phosphines and has been attributed to the presence of the lone electron pair at phosphorus as a reactive site [31]. After coordination to metal center, this reactive site is no longer available, which naturally simplifies the redox response. Indeed, the bis(chlorogold) complex **3** undergoes a standard, reversible one-electron oxidation (Fig. 9). Because of electron density transfer from the diphosphine ligand to the metal centers, this oxidation is more difficult than in **1**

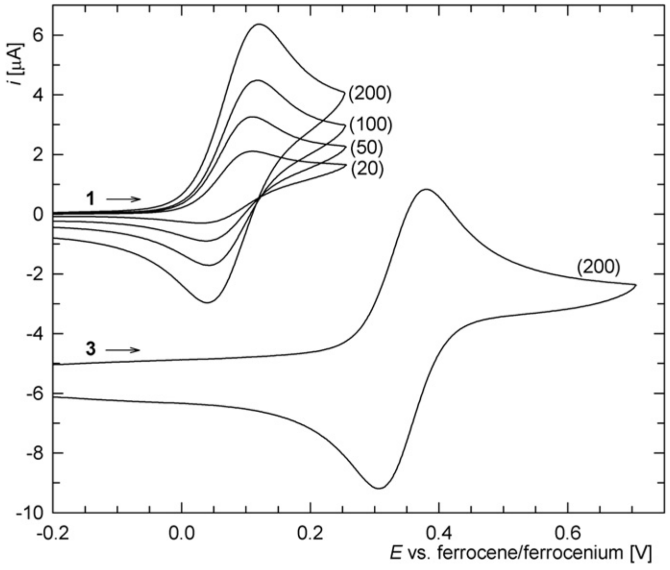

Fig. 9. Cyclic voltammograms of compounds **1** and **3** as recorded in dichloromethane at Pt disc electrode. The scan rate (in mV s^{-1}) is given in parentheses. The voltammogram of **3** is shifted by −5 μ along the *i*-axis to avoid overlaps and the scan direction is indicated with an arrow.

and the ferrocene/ferrocenium wave appears shifted toward higher potentials (by 0.33 V vs. **1**) [32]. Complexes **4** and **6** featuring other simple monoanionic ligands behave similarly (see Table 2).

The presence of redox-active pendant groups in **5** (FcC≡C) is noted by an additional reversible wave corresponding to two electrons exchanged at a potential similar to unsubstituted ferrocene (Fig. 10) [33]. The fact that both pendant ferrocenyl groups are oxidized in one step and that only a negligible change in the redox potential of the central ferrocene unit is observed as compared to **4** [34] rule out any significant electronic communication between the individual redox centers present in **5**. Finally, the redox response of compound **7** is complicated by additional redox changes (in addition to the $Fe^{II/III}$ wave) occurring presumably at the non-innocent dithiocarbamate ligands [35]. These redox processes generate a species, which is irreversibly reduced at 0.795 V (Fig. 11).

3. Conclusion

Compound **3**, readily prepared by the reaction of 1-(diphenylphosphino)-1′-[(diphenylphosphino)methyl]ferrocene with [AuCl(tht)], represents a good starting point for the synthesis of novel trimetallic Au_2Fe complexes via salt metathesis. It is noteworthy that unlike many compounds obtained analogously from the commonly used diphosphines (e.g., dppe or dppf), compound **3** and complexes derived thereof are not symmetric (i.e., composed of two equivalent parts) and thus suitable for investigation of the interactions between the metal centers and possible structural changes associated with modified structure by means of physicochemical methods and X-ray crystallography, respectively.

4. Experimental

4.1. Materials and methods

The syntheses were carried out under argon atmosphere and with exclusion of direct daylight. [AuCl(tht)] [36], **1** [14], and ethynylferrocene [37] were prepared according to the literature procedures. Dichloromethane and chloroform were dried over anhydrous potassium carbonate and distilled. Methanol was freshly distilled from sodium methoxide. Other chemicals and solvents used for crystallizations and chromatography were used as received (Fluka, Aldrich; solvents from Lachner).

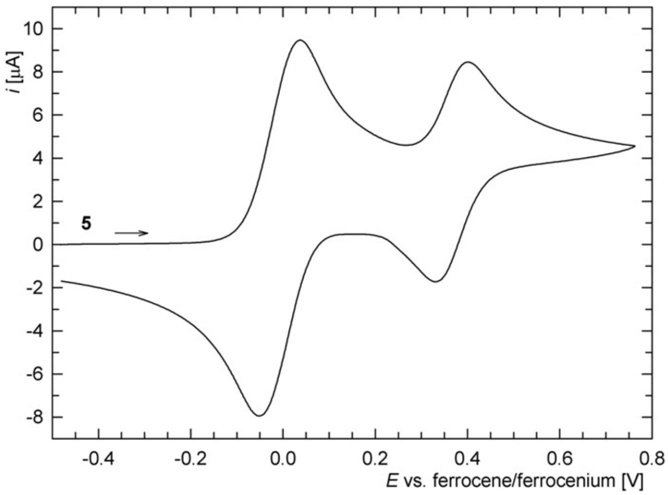

Fig. 10. Cyclic voltammogram of compound **5** (recorded in CH_2Cl_2 at Pt electrode, scan rate 200 mV s^{-1}). The scan direction is indicated with an arrow.

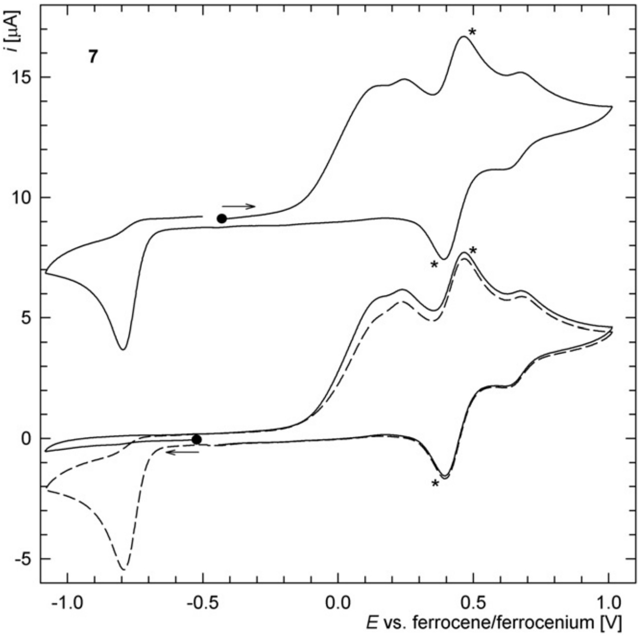

Fig. 11. Cyclic voltammetric response **7** in “oxidation first” (top) and “reduction first” (bottom) scans (in dichloromethane at Pt disc electrode, scan rate 200 mV s^{-1}). The starting potential and the scan direction are indicated with a filled circle and an arrow, respectively. In the “reduction first” scan (bottom), the second scan is shown by a dashed line. The asterisk indicates peaks tentatively attributed to the $Fe^{II/III}$ couple (the ferrocene unit). The voltammograms are shifted along the vertical axis to avoid overlaps.

NMR spectra were measured with a Varian UNITY Inova 400 spectrometer. Chemical shifts (δ/ppm) are given relative to internal $SiMe_4$ (^1H and ^{13}C) or to external 85% H_3PO_4 (^{31}P). In addition to the standard notation of signal multiplicity, vt and vq are used to denote virtual multiplets arising from AA′BB′ and AA′BB′X spin systems of the Ph_2PCH_2– and PPh_2–substituted cyclopentadienyl rings, respectively (Fc = ferrocenyl, fc = ferrocene-1,1′-diyl). IR spectra were recorded with an FTIR Nicolet Magna 760 instrument. UV–vis spectra were recorded on a Unicam UV 300 spectrometer for ca. 2×10^{-5} M solutions in dry 1,2-dichlorethane (Sigma–Aldrich, absolute). Electrospray ionization (ESI) mass spectra were obtained with a Bruker Esquire 3000 spectrometer. The samples were dissolved in a small amount of CH_2Cl_2 and then diluted with methanol in a large excess.

Electrochemical measurements were carried out with a computer-controlled potentiostat μAUTOLAB III (Eco Chemie, Netherlands) at room temperature (ca. 23 °C) using a Metrohm three-electrode cell equipped with a platinum disc working electrode (2 mm diameter), platinum sheet auxiliary electrode, and a double-junction Ag/AgCl (3 M KCl) reference electrode. The compounds were dissolved in dry dichloromethane (Sigma–Aldrich, absolute) to give a solution containing ca. 0.5–0.7 mM of the analyte and 0.1 M $Bu_4N[PF_6]$ (Fluka, puriss. for electrochemistry) as the supporting electrolyte. The solutions were deaerated with argon before the measurement and then kept under an argon blanket. The redox potentials (accuracy ca. 5 mV) were recorded relative to internal decamethylferrocene/decamethylferrocenium and then converted to the ferrocene/ferrocenium scale by subtracting 0.548 V [38].

4.2. In situ NMR study of the reaction between **1** and [AuCl(tht)]

Ligand **1** (11.5 mg, 0.020 mmol) and [AuCl(tht)] (6.5 mg, 0.020 mmol; molar ratio P:Au = 2:1) were dissolved in NMR grade

$CDCl_3$ (ca. 0.6 mL). The resulting solution was stirred for 30 min and analyzed by ^1H and $^{31}P\{^1H\}$ NMR spectroscopy. The solid product, which separated during storage of the reaction mixture at 4 °C overnight, was filtered off, washed with chloroform and dried under vacuum to afford compound **2** as a fine yellow solid. Yield: 14.6 mg (86%).

In situ ^1H NMR (400 MHz, $CDCl_3$, 25 °C): δ 1.94 (m, 4H, tht), 2.83 (m, 4H, tht), 3.75 (br s, 2H, CH_2), 3.90 (br s, 2H, fc), 4.22 (br s, 2H, fc), 4.32 (br s, 2H, fc), 4.61 (br s, 2H, fc), 7.32–7.69 (m, 20H, PPh_2). *In situ* $^{31}P\{^1H\}$ NMR (162 MHz, $CDCl_3$, 25 °C): δ 32.2, 37.0 (2× br s). Anal. calcd (%) for $C_{35}H_{30}AuClFeP_2 \cdot 0.3CHCl_3$ (836.6): C 50.68, H 3.65; found: C 50.43, H 3.64.

The reaction was performed also at P:Au molar ration of 1:1, i.e., with 13.0 mg (0.040 mmol) of [AuCl(tht)]. The ^1H and $^{31}P\{^1H\}$ NMR spectra of the reaction mixture revealed only the signals of complex **3** (see below) and free tht.

*4.3. Preparation of {μ-1κP:2κP′-1-(diphenylphosphino)-1′-[(diphenylphosphino)methyl]ferrocene}bis[chlorogold(I)] (**3**)*

A solution of **1** (57 mg, 0.10 mmol) in dichloromethane (3 mL) was added to solid [AuCl(tht)] (64.5 mg, 0.20 mmol). The resulting yellow–orange solution was stirred for 1 h and then precipitated with pentane (ca. 30 mL). During subsequent storing at 4 °C overnight, the amorphous precipitate converted into a microcrystalline solid, which was filtered off, washed with pentane and dried under vacuum to afford **3**$\cdot 0.25CH_2Cl_2$ as a bright yellow solid. Yield: 100 mg (95%).

^1H NMR (400 MHz, $CDCl_3$, 25 °C): δ 3.68 (d, $^2J_{PH} = 10.6$ Hz, 2H, CH_2), 3.88 (vt, $J' = 1.9$ Hz, 2H, fc), 4.21 (br d of vt, $J' \approx 0.5$, 1.9 Hz, 2H, fc), 4.24 (d of vt, $J' = 3.1$, 2.0 Hz, 2H, fc), 4.61 (m, 2H, fc), 7.38–7.84 (m, 20H, PPh_2). $^{31}P\{^1H\}$ NMR (162 MHz, $CDCl_3$, 25 °C): $\delta = 28.9$, 33.6 (2× s). MS (ESI+): *m/z* 1055 ($[M + Na]^+$), 997 ($[M - Cl]^+$), 765 ($[Au(\mathbf{1})]^+$). Anal. calcd (%) for $C_{35}H_{30}Au_2Cl_2FeP_2 \cdot 0.25CH_2Cl_2$ (1054.5): C 40.15, H 2.92; found: C 40.11, H 2.95.

*4.4. Preparation of {μ-1κP:2κP′-1-(diphenylphosphino)-1′-[(diphenylphosphino)methyl]ferrocene}bis[(phenylethynyl-κC^1) gold(I)] (**4**)*

A solution of ethynylbenzene (10.5 mg, 0.10 mmol) in absolute ethanol (3 mL) was treated with 0.1 M NaOEt in ethanol (2 mL, 0.20 mmol; prepared by dissolving sodium metal in absolute ethanol) while stirring and cooling in an ice bath. After 5 min, a solution of **3**$\cdot 0.25CH_2Cl_2$ (53 mg, 0.050 mmol) in dry dichloromethane (3 mL) was introduced, the cooling bath was removed, and the resulting cloudy yellow mixture was stirred at room temperature for 20 h. Then, it was evaporated under vacuum to give an orange residue, which was dissolved in dichloromethane (15 mL). The solution was washed with water (3 × 10 mL), dried over $MgSO_4$, and evaporated. The solid residue was washed with diethyl ether–pentane (1:1, 10 mL) and pentane (2 × 10 mL), and dried under vacuum. The crude product was dissolved in chloroform (ca. 3 mL) and the solution layered with absolute ethanol (ca. 7 mL). Subsequent crystallization by liquid-phase diffusion at room temperature and then at −18 °C over several days yielded an orange yellow crystalline solid, which was filtered off, washed with pentane and dried under vacuum. The crystals partly disintegrate upon work-up due to a loss of the clathrated solvent. Yield of **4**$\cdot 1.8CHCl_3$: 45 mg (65%).

^1H NMR (400 MHz, $CDCl_3$, 25 °C): δ 3.72 (d, $^2J_{PH} = 9.8$ Hz, 2H, CH_2), 3.86 (vt, $J' = 1.9$ Hz, 2H, fc), 4.23 (d of vt, $J = 2.8$, 2.0 Hz, 2H, fc), 4.32 (br vt, 2H, fc), 4.57 (d of vt, $J \approx 1.0$, 1.8 Hz, 2H, fc), 7.16–7.89 (m, 30H, PPh_2). $^{31}P\{^1H\}$ NMR (162 MHz, $CDCl_3$, 25 °C): δ 37.6, 40.3 (2× s). MS (ESI+): *m/z* 1380 (M^+), 1187 ($[M + Na]^+$), 1063 ($[M - PhC{\equiv}C]^+$), 765 ($[Au(\mathbf{1})]^+$). Anal. calcd (%) for $C_{51}H_{40}Au_2FeP_2 \cdot 1.8CHCl_3$ (1379.4): C 45.97, H 3.05; found: C 45.97, H 3.12.

*4.5. Preparation of {μ-1κP:2κP′-1-(diphenylphosphino)-1′-[(diphenylphosphino)methyl]ferrocene}bis[(ferrocenylethynyl-κC^1) gold(I)] (**5**)*

Ethynylferrocene (21 mg, 0.10 mmol) was dissolved in absolute ethanol (3 mL) with gentle warming. The solution was cooled in ice and then treated successively with 0.1 M NaOEt in ethanol (2 mL, 0.20 mmol) and a solution of **3**$\cdot 0.25CH_2Cl_2$ (53 mg, 0.050 mmol) in dry dichloromethane (3 mL). The cooling bath was removed and the resulting cloudy yellow–orange mixture was stirred at room temperature for 20 h and evaporated under vacuum. The orange residue was taken up with dichloromethane (15 mL), the solution was washed with water (3 × 10 mL), dried over $MgSO_4$, and evaporated. The solid residue was washed successively with diethyl ether–pentane (1:1, 10 mL) and pentane (2 × 10 mL), and dried under vacuum. The crude product was dissolved in chloroform (ca. 3 mL) and the solution was layered with absolute ethanol (ca. 9 mL). Crystallization at 4 °C for several days afforded a bright orange solid, which was filtered off, washed with pentane and dried under vacuum. Yield of **5**$\cdot 0.2CHCl_3$: 60 mg (85%).

^1H NMR (400 MHz, $CDCl_3$, 25 °C): δ 3.57 (d, $^2J_{PH} = 9.6$ Hz, 2H, CH_2), 3.88 (vt, $J' = 1.9$ Hz, 2H, fc), 4.09 (vt, $J' = 1.8$ Hz, 2H, C_5H_4 of Fc), 4.11 (vt, $J' = 1.9$ Hz, 2H, C_5H_4 of Fc), 4.21 (s, 10H, C_5H_5 of Fc), 4.22 (m, 2H, fc), 4.27 (br vt, 2H, fc), 4.35 (vt, $J' = 1.8$ Hz, 2H, C_5H_4 of Fc), 4.44 (vt, $J' = 1.9$ Hz, 2H, C_5H_4 of Fc), 4.55 (br d of vt, $J' = 0.9$, 1.9 Hz, 2H, fc), 7.36–7.81 (m, 20H, PPh_2). $^{31}P\{^1H\}$ NMR (162 MHz, $CDCl_3$, 25 °C): δ 37.6, 40.0 (2× s). MS (ESI+): *m/z* 1380 (M^+), 1403 ($[M + Na]^+$), 1419 ($[M + K]^+$), 1171 ($[M - FcC{\equiv}C]^+$), 765 ($[Au(\mathbf{1})]^+$). Anal. calcd (%) for $C_{59}H_{46}Au_2Fe_3P_2 \cdot 0.2CHCl_3$ (1404.3): C 50.63, H 3.46; found: C 50.77, H 3.52.

*4.6. Preparation of {μ-1κP:2κP′-1-(diphenylphosphino)-1′-[(diphenylphosphino)methyl]ferrocene}bis[(thiocyanato-κS) gold(I)] (**6**)*

Aqueous KSCN (19.5 mg, 0.20 mmol in 5 mL) was added to a solution of **3**$\cdot 0.25CH_2Cl_2$ (53 mg, 0.050 mmol) in dry dichloromethane (3 mL) and the resulting mixture was stirred vigorously for 18 h. The organic layer was separated and the aqueous phase was extracted with dichloromethane (2 × 5 mL). Combined organic layers were dried briefly over $MgSO_4$ and evaporated under vacuum. The residue was re-dissolved in dichloromethane (4 mL) and the solution was added to cold pentane (40 mL). After standing at 4 °C overnight, the precipitated product was filtered off, washed with pentane and dried under vacuum. Yield of **6**: 42 mg (78%), yellow solid.

^1H NMR (400 MHz, $CDCl_3$, 25 °C): δ 3.61 (d, $^2J_{PH} = 10.5$ Hz, 2H, CH_2), 3.97 (vt, $J' = 1.9$ Hz, 2H, fc), 4.23 (d of vt, $J = 0.8$, 1.9 Hz, 2H, fc), 4.30 (d of vt, $J = 3.0$, 1.9 Hz, 2H, fc), 4.63 (d of vt, $J = 1.2$, 1.8 Hz, 2H, fc), 7.43–7.70 (m, 20H, PPh_2). $^{31}P\{^1H\}$ NMR (162 MHz, $CDCl_3$, 25 °C): δ 33.7, 37.1 (2× s). MS (ESI+): *m/z* 765 ($[Au(\mathbf{1})]^+$); IR (Nujol): ν_{SCN} 2120 s, 2076 m cm^{-1}. Anal. calcd (%) for $C_{38}H_{36}Au_2FeP_2S_2$ (1068.5): C 41.20, H 2.80, N 2.60; found: C 41.28, H 2.89, N 2.51.

*4.7. Preparation of {μ-1κP:2κP′-1-(diphenylphosphino)-1′-[(diphenylphosphino)methyl]ferrocene}bis[(N,N-diethylcarbamodithioato-κS)gold(I)] (**7**)*

Aqueous solution of $NaS_2CNEt_2 \cdot 3H_2O$ (25 mg, 0.110 mmol in 5 mL) was added to a solution of **3**$\cdot 0.25CH_2Cl_2$ (53 mg, 0.050 mmol) in dichloromethane (5 mL), and the resulting heterogeneous mixture was vigorously stirred for 3 h. The organic layer was separated, washed with water (2 × 2 mL), shortly dried over $MgSO_4$ and evaporated. The residue was dissolved in dichloromethane (4 mL), treated with little charcoal, and filtered into pentane (40 mL). After standing at 4 °C overnight, the precipitated solid was filtered off and dried under vacuum to give **7** as a yellow solid. Yield: 52 mg (83%). Subsequent crystallization from chloroform–hexane afforded the stoichiometric solvate **7**·$CHCl_3$.

^1H NMR (400 MHz, $CDCl_3$, 25 °C): δ 1.32 (t, $^3J_{HH} = 7.1$ Hz, 12H, NCH_2CH_3), 3.63 (d, $^2J_{PH} = 10.0$ Hz, 2H, CH_2), 3.86 (vt, $J' = 1.9$ Hz, 2H, fc), 3.93 (q, $^3J_{HH} = 7.1$ Hz, 8H, NCH_2CH_3), 4.33 (d of vt, $J' \approx 2.9, 1.8$ Hz, 2H, fc), 4.41 (br d of vt, $J' \approx 0.7, 2.0$ Hz, 2H, fc), 4.53 (m, 2H, fc), 7.33–7.89 (m, 20H, PPh_2). $^{31}P\{^1H\}$ NMR (162 MHz, $CDCl_3$, 25 °C): δ 31.6, 34.8 (2× s); MS (ESI+): m/z 1110 ($[M - Et_2NCS_2]^+$). Anal. calcd (%) for $C_{45}H_{50}Au_2FeN_2P_2S_4 \cdot CHCl_3$ (1378.2): C 40.09, H 3.73, N 2.03; found: C 40.17, H 3.76, N 1.97.

4.8. Preparation of {μ-1κP:2κP′-1-(diphenylphosphino)-1′-[(diphenylphosphino)methyl]ferrocene}{μ-1κS:2κS′-propane-1,3-dithiolato}digold(I) (8)

Methanolic solution of sodium methoxide (1.1 mL 0.10 M, 0.11 mmol) was added to a solution of propane-1,3-dithiol (14 mg, 0.13 mmol) in the same solvent (10 mL). The mixture was stirred for ca. 5 min and then added drop-wise to a solution of **3**·$0.25CH_2Cl_2$ (53 mg, 0.050 mmol) in dichloromethane (10 mL) while stirring and cooling in ice. During the addition, the mixture became opaque. The cooling was removed and stirring was continued at room temperature for 20 h. The volatiles were removed under vacuum, and the yellow solid residue was partitioned between dichloromethane and water (20 mL each). The yellow organic extract was separated, dried over $MgSO_4$ and evaporated. The residue was taken up with chloroform (3 mL) and the solution layered with ethanol (8 mL). Crystallization by liquid-phase diffusion over several days afforded well-developed orange crystals, which were filtered off, washed with ethanol and dried under vacuum. Yield of **8**: 34 mg (64%), orange crystalline solid.

^1H NMR (400 MHz, $CDCl_3$, 25 °C): δ 2.51 (m, 2H, SCH_2CH_2), 2.79 (d, $^2J_{PH} = 10.1$ Hz, 2H, CH_2), 3.24 (br s, 4H, SCH_2), 4.18 (vt, $J' = 1.9$ Hz, 2H, fc), 4.27 (d of vt, $J = 2.9, 1.9$ Hz, 2H, fc), 4.47 (br vt, $J' \approx 1.7$ Hz, 2H, fc), 4.51 (d of vt, $J \approx 1.0, 1.8$ Hz, 2H, fc), 7.23–7.72 (m, 20H, PPh_2). $^{31}P\{^1H\}$ NMR (162 MHz, $CDCl_3$, 25 °C): δ 34.6, 37.7 (2× s). MS (ESI+): $m/z = 1069$ ($[M + H]^+$), 1091 ($[M + Na]^+$), 765 ($[Au(\mathbf{1})]^+$). Anal. calcd (%) for $C_{38}H_{36}Au_2FeP_2S_2$ (1068.5): C 42.71, H 3.40; found: C 42.35, H 3.19.

4.9. X-ray crystallography

Single-crystals suitable for X-ray diffraction measurements were grown by liquid-phase diffusion from 1,2-dichloroethane-diethyl ether (**3**·½$C_2H_4Cl_2$: yellow block, 0.30 × 0.35 × 0.40 mm^3; **8**: yellow plate, 0.15 × 0.18 × 0.20 mm^3), chloroform–ethanol (**4**·$2CHCl_3$: yellow prism, 0.03 × 0.13 × 0.25 mm^3), and from chloroform–pentane (**7**·$2CHCl_3$: yellow plate, 0.08 × 0.12 × 0.37 mm^3).

Full-set diffraction data ($\pm h \pm k \pm l$, $2\theta \le 55°$; completeness ≥99.7%) were collected with a Bruker Apex2 or a Nonius KappaCCD diffractometer equipped with Cryostream cooler (Oxford Cryosystems) using graphite-monochromated Mo Kα radiation ($\lambda = 0.71073$ Å). The data were corrected for absorption by methods included in the diffractometer software. Selected crystallographic data are summarized in Table 3.

The phase problems were solved by direct methods (SIR-97 [39] or SHELXS-97 [40]), and the structure models were refined by full-matrix least-squares based on F^2 (SHELXL-97 [40]). Unless specified otherwise, the non-hydrogen atoms were refined with anisotropic displacement parameters. The hydrogen atoms were included in their calculated positions and refined as riding atoms (SHELXL-97). One of the peripheral phenyl groups in the structure of compound **4**·$2CHCl_3$ was found to be disordered (slightly bent from the axis of the pivotal triple bond and rotated). It was modeled over two positions and refined with isotropic displacement parameters for the ring carbon atoms. Relative occupancies of the two contributing parts were refined to ca. 0.56 and 0.44.

All geometric calculations were performed with a recent version of PLATON program [41], which was also used to draw the Figures. All numerical values are rounded with respect to their estimated standard deviations given with one decimal.

Table 3
Crystallographic data, data collection and structure refinement parameters for **3**·½$C_2H_4Cl_2$, **4**·$2CHCl_3$, **7**·$2CHCl_3$, and **8**.[a]

Compound	**3**·½$C_2H_4Cl_2$	**4**·$2CHCl_3$	**7**·$2CHCl_3$	**8**
Formula	$C_{36}H_{32}Au_2Cl_3FeP_2$	$C_{53}H_{42}Au_2Cl_6FeP_2$	$C_{47}H_{52}Au_2Cl_6FeN_2P_2S_4$	$C_{38}H_{36}Au_2FeP_2S_2$
M	1082.69	1403.29	1497.57	1068.51
Crystal system	Monoclinic	Triclinic	Triclinic	Monoclinic
Space group	$C2/c$ (no. 15)	P–1 (no. 2)	P–1 (no. 2)	$P2_1/n$ (no. 14)
a (Å)	13.7584(2)	11.7993(1)	11.9439(2)	12.0071(1)
b (Å)	17.3175(2)	13.1519(1)	13.2821(2)	16.2432(3)
c (Å)	29.6625(3)	18.1798(2)	18.6206(3)	18.1711(3)
α (°)		85.2662(5)	87.5073(9)	
β (°)	94.0822(7)	76.1081(5)	74.4927(7)	105.357(1)
γ (°)		67.4502(5)	70.7019(9)	
V (Å^3)	7049.5(2)	2529.16(4)	2683.23(7)	3417.45(9)
Z	8	2	2	4
μ (Mo Kα) (mm^{-1})	9.053	6.485	6.270	9.227
T[b]	0.083–0.173	0.202–0.544	0.196–0.590	0.206–0.346
Diffrns collected	57,543	99,056	54,088	54,087
Independent diffrns	8096	11,649	12,271	7841
Observed[c] diffrns	7123	10,021	10,218	6469
R_{int}[d] (%)	8.43	6.63	4.49	5.65
R observed diffrns[c,d] (%)	3.22	3.15	2.72	2.58
R, wR[d] all data (%)	3.89, 8.25	4.02, 8.14	3.96, 5.74	3.73, 5.69
$\Delta\rho$ (e Å^{-3})	2.12, −1.97	1.76, −2.37	1.54, −1.27	0.87, −1.53

[a] Common details: $T = 150(2)$ K.

[b] The range of transmission factors.

[c] $I > 2\sigma(I)$.

[d] Definitions: $R_{int} = \sum|F_o^2 - F_o^2(\mathrm{mean})|/\sum F_o^2$, where F_o^2 (mean) is the average intensity of symmetry-equivalent diffractions. $R = \Sigma||F_o| - |F_c||/\Sigma|F_o|$, $wR = [\sum\{w(F_o^2 - F_c^2)^2\}/\sum w(F_o^2)^2 S]^{1/2}$.

Acknowledgements

This work was financially supported by the Czech Science Foundation (project no. P207/10/0176) and is a part of the long-term research plan of the Faculty of Science, Charles University in Prague supported by the Ministry of Education, Youth and Sports of the Czech Republic (project no. MSM0021620857).

Appendix A. Supporting material

CCDC 879017 (for **3**·½$C_2H_4Cl_2$), 879018 (for **4**·2$CHCl_3$), 879019 (for **7**·2$CHCl_3$) and 879020 (for **8**) contain the supplementary crystallographic data for this paper. These data can be obtained free of charge from The Cambridge Crystallographic Data Centre via www.ccdc.cam.ac.uk/data_request/cif.

References

[1] (a) M.C. Gimeno, A. Laguna, in: J.A. McCleverty, T.J. Meyer (Eds.), Comprehensive Coordination Chemistry II, vol. 6, Elsevier, Oxford, 2004, pp. 911–1145 (chapter 6.7);
(b) M.C. Gimeno, in: A. Laguna (Ed.), Modern Supramolecular Gold Chemistry: Gold-Metal Interactions and Applications, Wiley-VCH, Weinheim, 2008, pp. 1–63 (chapter 1).

[2] Selected reviews (a) H. Schmidbaur, A. Schier, Chem. Soc. Rev. 41 (2012) 370–412;
(b) H. Schmidbaur, S. Cronje, B. Djordjevic, O. Schuster, Chem. Phys. 311 (2005) 151–161;
(c) H. Schmidbaur, A. Schier, Chem. Soc. Rev. 37 (2008) 1931–1951;
(d) H. Schmidbaur, Gold Bull. 33 (2000) 3–10;
(e) P. Pyykkö, Angew. Chem. Int. Ed. 43 (2004) 4412–4456.

[3] (a) V.W.-W. Yam, E.C.-C. Cheng, Chem. Soc. Rev. 37 (2008) 1806–1813;
(b) E.R.T. Tiekink, J.-G. Kang, Coord. Chem. Rev. 253 (2009) 1627–1648;
(c) J.C. Lima, L. Rodríguez, Chem. Soc. Rev. 40 (2011) 5442–5456;
(d) X. He, V.W.-W. Yam, Coord. Chem. Rev. 255 (2011) 2111–2123.

[4] (a) A.S.K. Hashmi, M. Rudolph, Chem. Soc. Rev. 37 (2008) 1766–1775;
(b) N. Marion, S.P. Nolan, Chem. Soc. Rev. 37 (2008) 1776–1782;
(c) Z. Li, C. Brouwer, C. He, Chem. Rev. 108 (2008) 3239–3265;
(d) A. Arcadi, Chem. Rev. 108 (2008) 3266–3325;
(e) A. Pradal, P.Y. Toullec, V. Michelet, Synthesis (2011) 1501–1514;
(f) M. Rudolph, A.S.K. Hashmi, Chem. Soc. Rev. 41 (2012) 2448–2462.

[5] (a) M.J. McKeage, L. Maharaj, S.J. Berners-Price, Coord. Chem. Rev. 232 (2002) 127–135;
(b) E.R.T. Tiekink, Inflammopharmacol 16 (2008) 133–142;
(c) I. Ott, Coord. Chem. Rev. 253 (2009) 1670–1681;
(d) M. Navarro, Coord. Chem. Rev. 253 (2009) 1619–1626;
(e) H.E. Abdou, A.A. Mohamed, J.P. Fackler Jr., A. Burini, R. Galassi, J.M. López-de-Luzuriaga, M.E. Olmos, Coord. Chem. Rev. 253 (2009) 1661–1669;
(f) A. Bindoli, M.P. Rigobello, G. Scutari, C. Gabbiani, A. Casini, L. Messori, Coord. Chem. Rev. 253 (2009) 1692–1707;
(g) J.C. Lima, L. Rodriguez, Anti-Cancer Agents Med. Chem. 11 (2011) 921–928.

[6] R.J. Puddephatt, Chem. Soc. Rev. 37 (2008) 2012–2027.

[7] Selected examples (a) D.T. Hill, G.R. Girard, F.L. McCabe, R.K. Johnson, P.D. Stupik, J.H. Zhang, W.M. Reiff, D.S. Eggleston, Inorg. Chem. 28 (1989) 3529–3533;
(b) A. Houlton, R.M.G. Roberts, J. Silver, R.V. Parish, J. Organomet. Chem. 418 (1991) 269–275;
(c) L.T. Phang, S.C.F. Au-Yeung, T.S.A. Hor, S.B. Khoo, Z.Y. Zhou, T.C.W. Mak, J. Chem. Soc. Dalton Trans. (1993) 165–172;
(d) P.M.N. Low, Y.K. Yan, H.S.O. Chan, T.S.A. Hor, J. Organomet. Chem. 454 (1993) 205–209;
(e) M.C. Gimeno, A. Laguna, C. Sarroca, P.G. Jones, Inorg. Chem. 32 (1993) 5926–5932;
(f) A. Houlton, D.M.P. Mingos, D.M. Murphy, D.J. Williams, L.T. Phang, T.S.A. Hor, J. Chem. Soc. Dalton Trans. (1993) 3629–3630;
(g) L.T. Phang, T.S.A. Hor, Z.-Y. Zhou, T.C.W. Mak, J. Organomet. Chem. 469 (1994) 253–261;
(h) F. Canales, M.C. Gimeno, A. Laguna, P.G. Jones, J. Am. Chem. Soc. 118 (1996) 4839–4845;
(i) V.W.-W. Yam, S.W.-K. Choi, K.-K. Cheung, J. Chem. Soc. Dalton Trans. (1996) 3411–3415;
(j) P.M.N. Low, Z.-Y. Zhang, T.C.W. Mak, T.S.A. Hor, J. Organomet. Chem. 539 (1997) 45–51;
(k) M.J. Calhorda, F. Canales, M.C. Gimeno, J. Jimenez, P.G. Jones, A. Laguna, L.F. Veiros, Organometallics 16 (1997) 3837–3844;
(l) F. Canales, M.C. Gimeno, P.G. Jones, A. Laguna, C. Sarroca, Inorg. Chem. 36 (1997) 5206–5211;
(m) O. Crespo, F. Canales, M.C. Gimeno, P.G. Jones, A. Laguna, Organometallics 18 (1999) 3142–3148;
(n) J.D.E.T. Wilton-Ely, A. Schier, N.W. Mitzel, H. Schmidbaur, J. Chem. Soc. Dalton Trans. (2001) 1058–1062;
(o) J.D.E.T. Wilton-Ely, A. Schier, N.W. Mitzel, S. Nogai, H. Schmidbaur, J. Organomet. Chem. 643–644 (2002) 313–323;
(p) V.W.-W. Yam, K.-L. Cheung, E.C.-C. Cheng, N. Zhu, K.-K. Cheung, Dalton Trans. (2003) 1830–1835;
(q) L. Song, S.-Q. Xia, S.-M. Hu, S.-W. Du, X.-T. Wu, Polyhedron 24 (2005) 831–836;
(r) W. Henderson, B.K. Nicholson, E.R.T. Tiekink, Inorg. Chim. Acta 359 (2006) 204–214;
(s) P. Teo, L.L. Koh, T.S.A. Hor, Chem. Commun. (2007) 2225–2227;
(t) M. Ferrer, A. Gutierrez, L. Rodriguez, O. Rossell, J.C. Lima, M. Font-Bardia, X. Solans, Eur. J. Inorg. Chem. (2008) 2899–2909;
(u) E.R. Knight, N.H. Leung, A.L. Thompson, G. Hogarth, J.D.E.T. Wilton-Ely, Inorg. Chem. 48 (2009) 3866–3874.

[8] (a) S.W. Chien, T.S.A. Hor, in: P. Štěpnička (Ed.), Ferrocenes: Ligands, Materials and Biomolecules, Wiley, Chichester, 2008. pp. 33–116;
(b) K.-S. Gan, T.S.A. Hor, in: A. Togni, T. Hayashi (Eds.), Ferrocenes: Homogeneous Catalysis, Organic Synthesis Materials Science, Wiley-VCH, Weinheim, 1995. pp. 3–104;
(c) G. Bandoli, A. Dolmella, Coord. Chem. Rev. 209 (2000) 161–196.

[9] (a) K. Roessler, T. Rueffer, B. Walfort, R. Packheiser, R. Holze, M. Zharnikov, H. Lang, J. Organomet. Chem. 692 (2007) 1530–1545;
(b) R. Packheiser, A. Jakob, P. Ecorchard, B. Walfort, H. Lang, Organometallics 27 (2008) 1214–1226.

[10] E.M. Barranco, O. Crespo, M.C. Gimeno, A. Laguna, P.G. Jones, B. Ahrens, Inorg. Chem. 39 (2000) 680–687.

[11] N.J. Goodwin, W. Henderson, Polyhedron 17 (1998) 4071–4077.

[12] (a) A. Jakob, P. Ecorchard, M. Linseis, R.F. Winter, H. Lang, J. Organomet. Chem. 694 (2009) 655–666;
(b) E. Fourie, E. Erasmus, J.C. Swarts, A. Jakob, H. Lang, G.K. Joone, C.E.J. Van Rensburg, Anticancer Res. 31 (2011) 825–830.

[13] (a) U. Siemeling, T. Klemann, C. Bruhn, J. Schulz, P. Štěpnička, Z. Anorg. Allg. Chem. 637 (2011) 1824–1833;
(b) P. Štěpnička, M. Zábranský, I. Císařová, ChemistryOpen 1 (2012) 71–79.

[14] P. Štěpnička, I. Císařová, J. Schulz, Organometallics 30 (2011) 4393–4403.

[15] M. Viotte, B. Gautheron, M.M. Kubicki, Y. Mugnier, R.V. Parish, Inorg. Chem. 34 (1995) 3465–3473.

[16] M. Viotte, B. Gautheron, I. Nifant'ev, L.G. Kuz'mina, Inorg. Chim. Acta 253 (1996) 71–76.

[17] (a) F.R. Hartley, Chem. Soc. Rev. 2 (1973) 163–179;
(b) B.J. Coe, S.J. Glenwright, Coord. Chem. Rev. 203 (2000) 5–80.

[18] D. Schneider, S. Nogai, A. Schier, H. Schmidbaur, Inorg. Chim. Acta 352 (2003) 179–187.

[19] O. Crespo, M.C. Gimeno, P.G. Jones, A. Laguna, Acta Crystallogr. Sect. C 56 (2000) 1433–1434.

[20] U. Siemeling, D. Rother, C. Bruhn, Organometallics 27 (2008) 6419–6426.

[21] J.G. Wijnhoven, W.P.J.H. Bosman, P.T. Beurskens, J. Cryst. Mol. Struct. 2 (1972) 7–15.

[22] S.Y. Ho, E.R.T. Tiekink, Acta Crystallogr. Sect. E 58 (2002) m86–m87.

[23] J.W. Faamau, E.R.T. Tiekink, J. Coord. Chem. 31 (1994) 93–101.

[24] G. Hogart, Progr. Inorg. Chem. 53 (2005) 71–561.

[25] Data from the Cambridge Crystallographic Data Centre, http://www.ccdc.cam.ac.uk/products/csd/radii/table.php4 (retrieved on 10.04.12).

[26] Rather similar Au–S/S′ distances (2.969(4) and 2.319(4) Å) but clearly distinguishable C=S/C–S bond lengths (1.66(1) and 1.77(1) Å) can be found in $[(\mu\text{-}H_2C)C(PPh_2)_2)\{Au(dtc)\}_2]$: E.J. Fernández, J.M. López-de-Luzuriaga, M. Monge, E. Olmos, M.C. Gimeno, A. Laguna, P.G. Jones Inorg. Chem. 37 (1998) 5532–5536.

[27] The signs of the torsion angles C7–C6–C11–P2, C6–C11–P2–Au2 and C5–C1–P1–Au1 for compounds **3**·½$C_2H_4Cl_2$, **4**·2$CHCl_3$ and **7**·2$CHCl_3$ reflect only the choice of the structurally independent part. Upon inversion (allowed in these centrosymmetric structures) the signs are inverted, too. Hence, it is only their mutual relationship what matters.

[28] Similar parameters were reported also for $[(\mu\text{-dppf})(AuSPh)_2]$ (Au–S 2.316(9) Å, Au–P 2.274(8) Å, P–Au–S 170.7(3)°) and compounds modified at the benzenethiolato ligand (a) S. Onaka, Y. Katsukawa, M. Shiotsuka, O. Kanegawa, M. Yamashita, Inorg. Chim. Acta 312 (2001) 100–110;
(b) D.R. Smyth, J. Hester, V.G. Young Jr., E.R.T. Tiekink, CrystEngComm 4 (2002) 517–521.

[29] The dihedral angle P1–Au1–Au2–P2 in **8** is $-17.06(4)^\circ$.

[30] Rather unexpectedly, crystalline **8** does not dissolve appreciably in dichloromethane even after gentle warming and sonification

[31] Selected examples (a) G. Pilloni, B. Longato, B. Corain, J. Organomet. Chem. 420 (1991) 57–65;
(b) P. Zanello, G. Opromolla, G. Giorgi, G. Sasso, A. Togni, J. Organomet. Chem. 506 (1996) 61–65;
(c) J. Podlaha, P. Štěpnička, J. Ludvík, I. Císařová, Organometallics 15 (1996) 543–550;
(d) B.L. Ghent, S.L. Martinak, L.A. Sites, J.A. Golen, A.L. Rheingold, C. Nataro, J. Organomet. Chem. 692 (2007) 2365–2374.

[32] Anodic shift as high as 0.41 V was observed upon going from dppf to $[(\mu\text{-dppf})(AuCl)_2]$: S.L. Kahn, M.K. Breheney, S.L. Martinak, S.M. Fosbenner, A.R. Seibert, W.S. Kassel, W.G. Dougherty, C. Nataro, Organometallics 28 (2009) 2119–2126.

[33] Ethynylferrocene becomes oxidized at slightly more positive potentials (a) P. Štěpnička, R. Gyepes, O. Lavastre, P.H. Dixneuf, Organometallics 16 (1997) 5089–5095;
(b) P. Štěpnička, L. Trojan, J. Kubišta, J. Ludvík, J. Organomet. Chem. 637–639 (2001) 291–299.
[34] The first oxidation step generates a dication 5^{2+} which should be (in principle) more difficult to oxidize than the neutral compound **4**. Besides, the terminal substituents (Ph vs. Fc) can be expected to have a minor influence on the oxidation of the central ferrocene unit.
[35] A.M. Bond, R.L. Martin, Coord. Chem. Rev. 54 (1984) 23–98.
[36] R. Uson, A. Laguna, M. Laguna, Inorg. Synth. 26 (1989) 85–91.
[37] M. Rosenblum, N. Brawn, J. Papenmeier, M. Applebaum, J. Organomet. Chem. 6 (1966) 173–180.
[38] F. Barrière, W.E. Geiger, J. Am. Chem. Soc. 128 (2006) 3980–3989.
[39] A. Altomare, M.C. Burla, M. Camalli, G.L. Cascarano, C. Giacovazzo, A. Guagliardi, A.G.G. Moliterni, G. Polidori, R. Spagna, J. Appl. Crystallogr. 32 (1999) 115–119.
[40] G.M. Sheldrick, Acta Crystallogr. Sect. A 64 (2008) 112–122.
[41] A.L. Spek, J. Appl. Crystallogr. 36 (2003) 7–13.